Published for SISSA by Springer

Received: May 4, 2023
Accepted: June 13, 2023
Published: June 26, 2023

Time-like entanglement entropy in AdS/BCFT

Chong-Sun Chu[a,b,c] **and Himanshu Parihar**[b,c]

[a] *Department of Physics, National Tsing-Hua University, Hsinchu 30013, Taiwan*

[b] *Center of Theory and Computation, National Tsing-Hua University, Hsinchu 30013, Taiwan*

[c] *Physics Division, National Center for Theoretical Sciences, Taipei 10617, Taiwan*

E-mail: cschu@phys.nthu.edu.tw, himansp@phys.ncts.ntu.edu.tw

Abstract: We study the entanglement entropy for time-like subsystem in two-dimensional boundary conformal field theory (BCFT) both from the field theory and holographic point of view. In field theory, we compute the time-like entanglement entropy of a pure time-like interval at zero and finite temperature using the replica technique and analytical continuation. We find that, similar to the ordinary space-like entanglement entropy in BCFT, the time-like entropy also has a bulk phase and a boundary phase which corresponds respectively to the dominance of the identity block in the bulk and boundary OPE channels. However, we find that in Lorentzian BCFT, the time-like entanglement entropy posses a third *Regge phase* which arises in the Regge limit of the interval, when one endpoint of the time interval approaches the light cone of the mirror image of the other endpoint. We determine the phase diagram for the time-like entanglement entropy. We find that while the time-like entropy is complex in the bulk phase and has a boundary term in the boundary phase, there is no boundary entropy in the Regge phase. Moreover, it can be real or complex depending on which side the Regge limit is approached from. On the gravity side, we obtain the holographic time-like entanglement entropy from the corresponding bulk dual geometries and find exact agreement with the field theory results. The time-like entanglement entropy may be useful to describe the entanglement of a quantum dot on a half line.

Keywords: AdS-CFT Correspondence, Gauge-Gravity Correspondence

ArXiv ePrint: 2304.10907

https://doi.org/10.1007/JHEP06(2023)173

Contents

1 Introduction

The AdS/CFT correspondence [1] provides an interesting relation between the d dimensional conformal field theory (CFT) to that of quantum gravity on a $(d+1)$ asymptotically anti-de Sitter (AdS) spacetime. One can extend the AdS/CFT to the case where a CFT is defined on a manifold with boundaries (e.g. CFT on a half plane). This class of CFTs with a boundary is called a boundary conformal field theory (BCFT) when a part of conformal symmetry (called boundary conformal symmetry) is preserved at the boundary [2–6]. The holographic dual of such BCFTs are given by an asymptotically AdS spacetime truncated by an end of the world (EOW) brane which satisfy either the Neumann boundary condition [7, 8] as it was originally proposed, the conformal boundary condition [9, 10] or the Dirichlet boundary condition [11] which were found later to all define consistent holographic BCFT.

Owed to discovery of the Ryu-Takayanagi (RT) formula [12, 13] for the entanglement entropy for bipartite pure states, the holographic study of quantum entanglement has become one of the most active recent developments of AdS/CFT. The entanglement entropy for such bipartite states can be obtained in a $(1+1)$ dimensional conformal field theories using a replica technique [14, 15]. The holographic entanglement entropy of a subregion A in a dual CFT may be computed in terms of the area of the codimension two extremal surface (Γ_A) homologous to the boundary subregion as

$$S_A = \frac{\text{Area}(\Gamma_\text{A})}{4G_N}. \tag{1.1}$$

This formula becomes more interesting in AdS/BCFT since the minimal surface can now end on the EOW brane as first noted in [7, 8]. Moreover, depending on the position of the interval A from the boundary, there will be competition between the bulk minimal surface and the minimal surface that ends on the EOW brane and give rises to a phase transition of the entanglement entropy since the two surfaces have different topology [9, 10]. In field theory, this corresponds to the shift from the vacuum block dominance in the OPE of the bulk channel OPE to the boundary channel [16].

Recently, the authors of [17] proposed a new quantity for the entanglement measure for a time-like subsystem known as the *time-like entanglement entropy*.[1] It is defined by analytically continuing the entanglement entropy of a space-like subsystem A to the case where the subsystem A becomes a time-like subsystem. The time-like entanglement entropy (TEE) is found to have a complex value in a CFT_2. Furthermore, it was shown that the extremal surface for the holographic TEE consists of space-like and time-like parts which give rises to the real part and the imaginary part of the time-like entanglement entropy respectively. It was also argued that [17, 19] the TEE is a special example of pseudo entropy [20–22]. See [23–38] for recent progress related to TEE.

The above developments lead naturally to an interesting question about the time-like entanglement entropy in BCFT. In fact, from the point of view of BCFT and replica technique, the bulk phase and boundary phase of the entanglement entropy arises from the vacuum block dominance in the bulk and boundary channel of the OPE of the twist operators, which occurs in the bulk limit ($\xi \to 0$) and the boundary limit ($\xi \to \infty$) respectively. Here ξ is the cross ratio for the two endpoints of the interval together with their images. Now in a Lorentzian BCFT, the two point function is known to have a branch point singularity in the Regge limit $\xi \to -1$ [39], which arises when one endpoint of the time interval approaches the light-cone of the mirror image of the other endpoint.[2] Therefore, in addition to the bulk and boundary limits, one can expect to find new interesting properties for the TEE in the Regge limit of BCFT. The study of this richer phase structure of TEE in BCFT is one of the main motivations of this paper. We find that unlike the usual space-like entropy which consists of a bulk phase and a boundary phase, the TEE in BCFT has a new third phase which arises in the Regge limit of the time-like interval. An interesting novel feature here is that the TEE goes from real value to complex as the time interval goes pass the Regge limit point.

This article is organized as follows. In section 2 we briefly review about the time-like entanglement entropy in AdS_3/CFT_2. In section 3 we review some of the salient features of BCFT. In section 4 we obtain the time-like entanglement entropy of a pure time-like interval at zero and finite temperature in a $BCFT_2$. We identify the Regge phase and determine the phase diagram for the TEE. In section 5 we compute the time-like entanglement entropy using $AdS_3/BCFT_2$. The RT surface in the bulk phase consists of space-like and time-like geodesics leading to a complex valued TEE. In the boundary phase, the RT surface consists of two geodesics ending on the EOW brane and it gives a real valued TEE. Finally, the

[1] Note that it has been introduced earlier in the context of $T\bar{T}$ deformed version of the AdS_3/CFT_2 correspondence in [18].

[2] We remark that the Regge limit, and hence the Regge phase of the TEE, is possible only in BCFT when the interval is time-like.

RT surface in the Regge phase is given by the geodesic joining the end point of interval and ending on the plane perpendicular to the boundary. The geodesics lie along the plane crossing one end point of the interval and mirror reflection of the other end point of the interval. Remarkably, we obtain exact matches between the field theory replica technique results and the bulk holographic computation of the TEE. Finally in section 6 we present our summary and discussions.

2 Time-like entanglement entropy in AdS_3/CFT_2

In this section, we briefly review the time-like entanglement entropy for the configuration of a time-like interval in AdS_3/CFT_2 framework [17]. Consider a generic space-like interval $A \equiv [(t_1, x_1), (t_2, x_2)]$ in a CFT_2 whose time-like and space-like width are given by $t_{12} = T_0$ and $x_{12} = X_0$ respectively. Then, the entanglement entropy S_A of an interval A may be obtained using the replica technique as [14, 15]

$$S_A = \frac{c}{3} \log \frac{\sqrt{X_0^2 - T_0^2}}{\epsilon}, \tag{2.1}$$

where ϵ is a UV cut-off and c is the central charge of the CFT. The time-like entanglement entropy S_A^T for a purely time-like interval A is obtained by analytically continuing the space-like interval to a time-like interval followed by taking $X_0 = 0$ in eq. (2.1) as follows [17]

$$S_A^T = \frac{c}{3} \log \left(\frac{T_0}{\epsilon} \right) + \frac{i\pi c}{6}. \tag{2.2}$$

It is observed that the above TEE takes complex values for the standard unitary CFTs.

At finite temperature $T = 1/\beta$, the entanglement entropy for a generic space-like interval of width t_{12} and x_{12} at finite temperature is obtained by evaluating the two point twist correlator on a cylinder of circumference β and the result is [14, 15]

$$S_A = \frac{c}{6} \log \left[\frac{\beta^2}{\pi^2 \epsilon^2} \sinh \left(\frac{\pi}{\beta} (x_{12} + t_{12}) \right) \sinh \left(\frac{\pi}{\beta} (x_{12} - t_{12}) \right) \right]. \tag{2.3}$$

Then, the time-like entanglement entropy for a purely time-like interval at finite temperature can be computed by taking $x_{12} = 0$ and $t_{12} = T_0$ in eq. (2.3) as follows [17]

$$S_A^T = \frac{c}{3} \log \left[\frac{\beta}{\pi \epsilon} \sinh \frac{\pi T_0}{\beta} \right] + \frac{i\pi c}{6}. \tag{2.4}$$

The above result for TEE at finite temperature also have complex value similar to the zero temperature case.

Next we review the holographic time-like entanglement entropy of a time-like interval in the AdS_3/CFT_2 scenario [17]. To this end, consider the Poincaré patch of a AdS_3 spacetime (with AdS radius $R_{\mathrm{AdS}} = 1$) whose metric is given by

$$ds^2 = \frac{dz^2 - dt^2 + dx^2}{z^2}. \tag{2.5}$$

The time-like interval A of the boundary CFT_2 has finite width T_0 along the time direction and fixed spatial coordinate in x direction described by $x_1 = x_2$. It is argued in [17] that due to the lack of space-like geodesic connecting the boundary of time-like interval A, one should use two space-like geodesics connecting the endpoints of A and null infinities followed by a time-like geodesic which connects the endpoints of two space-like geodesics. The holographic time-like entanglement entropy for the time-like interval is then given by the length of these three geodesics. The equation for the space-like geodesic which connects endpoints ∂A with null infinities is given by

$$t = \sqrt{z^2 + T_0^2/4}, \tag{2.6}$$

which can identified as a semi-circle geodesic via the Wick rotation. On utilizing the RT formula, the time-like entanglement entropy is given by the length of this space-like geodesic as

$$S_A^T = \frac{1}{4G_N} 2T_0 \int_\epsilon^\infty \frac{dz}{2z\sqrt{z^2 + T_0^2/4}} = \frac{c}{3} \log \frac{T_0}{\epsilon}, \tag{2.7}$$

where $c = \frac{3}{2G_N}$ is used [40]. It matches with the real part of the dual CFT_2 result in eq. (2.2). The imaginary part of the time-like entanglement entropy is obtained by embedding the Poincaré patch in the global patch whose metric is given by

$$ds^2 = -\cosh^2 \rho d\tau^2 + d\rho^2 + \sinh^2 \rho d\theta^2. \tag{2.8}$$

Then, the imaginary part is given by the length of a time-like geodesic connecting two endpoints at $\rho = 0$ and $\tau = \pm\frac{\pi}{2}$ in the global coordinates. The length of this time-like geodesic is $\pi c/6$ which matches with the imaginary part of dual CFT_2 result as described in eq. (2.2).

For the time-like interval A of length T_0 at a finite temperature, the gravity dual is described by the planar BTZ black hole whose metric (with $R_{\mathrm{AdS}} = 1$) is given by

$$ds^2 = -\left(r^2 - r_+^2\right) dt^2 + \frac{dr^2}{r^2 - r_+^2} + r^2 dx^2, \tag{2.9}$$

where $r_+ = \frac{2\pi}{\beta}$ and β is the inverse temperature of the dual CFT_2. Similarly, the time-like entanglement entropy for a time-like interval A at a finite temperature is given by the length of space-like and time-like extremal surfaces in the BTZ black hole background which can be expressed as [17]

$$S_A^T = \frac{c}{3} \log \left[\frac{\beta}{\pi\epsilon} \sinh\left(\frac{\pi T_0}{\beta}\right)\right] + \frac{i\pi c}{6}, \tag{2.10}$$

which agrees with the corresponding dual field theory result (2.4).

3 Review of BCFT

In this section, we will briefly review the salient features of the boundary conformal field theories [2, 6, 39, 41]. A boundary conformal field theory (BCFT) is a conformal field theory (CFT) defined on a manifold with boundaries such that a part of conformal symmetry is preserved by the boundaries. There are many different possible choices of conformal-invariant boundary conditions for a given CFT. When the BCFT_d lives on the half-plane $\mathbb{R}^{d-1}\times\mathbb{R}_+$ with a planar boundary, a BCFT_d has the symmetry $\mathrm{SO}(d-1,2)$ in Lorentzian signature (or $\mathrm{SO}(d,1)$ in Euclidean signature) which is the subgroup of original CFT_d symmetry group.

Consider a BCFT in d dimension space with a time independent planar boundary. Denote the coordinates by $x = (x_0, \vec{x}, x_\perp)$ where x_0 is the time coordinate, $\vec{x}$ are the Euclidean coordinates parallel to the boundary and $x_\perp$ is orthogonal to the boundary. The one-point function in a BCFT behaves kinematically like a CFT two-point function which is given by [2]

$$\langle \mathcal{O}(x)\rangle = \frac{A_{\mathcal{O}}}{(2x_\perp)^\Delta}, \tag{3.1}$$

where the coefficient $A_{\mathcal{O}}$ is a physical parameter depending on both the operator and the boundary condition, and Δ is the scaling dimension of the operator $\mathcal{O}$. Similarly, the two-point function of scalar operators in a BCFT behaves kinematically like a CFT four-point function

$$\langle \mathcal{O}(x)\mathcal{O}(y)\rangle = \frac{1}{|4x_\perp y_\perp|^\Delta}\mathcal{G}(\xi)\ , \tag{3.2}$$

and depends on an undetermined function of a single conformal-invariant cross-ratio ξ

$$\xi = \frac{(x-y)^2}{4x_\perp y_\perp} = \frac{\pm(x_0-y_0)^2 + (\vec{x}-\vec{y})^2 + (x_\perp - y_\perp)^2}{4x_\perp y_\perp}. \tag{3.3}$$

Here the $+$ sign is for the Euclidean theory and the $-$ sign is for the Lorentzian theory. The cross ratio ξ takes positive values when the two operators live in the Euclidean signature or are space-like separated in the Lorentzian signature. The two point correlation function in a BCFT can be expanded in two different OPE limits namely the bulk limit $\xi \to 0$ and the boundary limit $\xi \to \pm\infty$[3] as

$$\mathcal{G}(\xi) = \sum_{\mathcal{O}} \lambda_{\mathcal{O}} g^B_{\Delta_{\mathcal{O}}}(\xi) = \sum_{\hat{\mathcal{O}}} \mu_{\hat{\mathcal{O}}} g^b_{\Delta_{\hat{\mathcal{O}}}}(\xi), \tag{3.4}$$

where g^B and g^b are the bulk and boundary conformal blocks respectively, and the sum is over the set of bulk primary operators $\mathcal{O}$ or boundary primary operators $\hat{\mathcal{O}}$ which appear in the corresponding OPEs.

The Euclidean BCFT correlation function have singularities only when the operators approach each other or when they approach the boundary (which can be thought as an operator approaching their mirrored double across the boundary). When the two operators approach each other and away from the boundary, the BCFT two-point function in the bulk limit $\xi \to 0$ behaves like [41]

$$\langle \mathcal{O}(x)\mathcal{O}(y)\rangle = \frac{1}{|x-y|^{2\Delta}} + \dots, \quad \mathcal{G}(\xi) \sim \xi^{-\Delta}, \qquad \text{as } \xi \to 0. \tag{3.5}$$

[3] In Euclidean signature, the boundary limit is given by $\xi \to \infty$. In Lorentzian signature and for a time-like interval, it is also possible to reach the boundary in the limit of $\xi \to -\infty$.

Similarly, the two point BCFT correlator in the boundary limit $\xi \to \infty$ when the operators are much closer to the boundary than to each other, the correlator behaves like [41]

$$\langle \mathcal{O}(x)\mathcal{O}(y)\rangle = \frac{\mathcal{A}^2}{|4x_\perp y_\perp|^\Delta} + \ldots, \quad \mathcal{G}(\xi) \sim \mathcal{A}^2, \qquad \text{as } \xi \to \infty \tag{3.6}$$

for some constant $\mathcal{A}$. When the operators $\mathcal{O}(x)$ and $\mathcal{O}(y)$ are time-like separated in the Lorentzian signature, the two point function can be obtained by an analytic continuation of $\mathcal{G}(\xi)$ to the time-like region $\xi < 0$ around the branch-point at $\xi = 0$. Then, there exists another singularity in the limit $\xi = -1$, known as Regge limit of the BCFT [39] where $\mathcal{O}(y)$ approaches the light-cone of the mirror reflection of $\mathcal{O}(x)$ with the boundary behaving like the mirror. The BCFT two point function diverges at the Regge limit $\xi \to -1$ as [39, 41]

$$\langle \mathcal{O}(x)\mathcal{O}(y)\rangle = \frac{1}{|4x_\perp y_\perp|^\Delta}\frac{1}{(1+\xi)^\Delta} + \ldots, \quad \mathcal{G}(\xi) \sim (\xi+1)^{-\Delta}, \qquad \text{as } \xi \to -1. \tag{3.7}$$

As shown in [42], a CFT correlation function have singularities at the location of the Landau diagrams where null particles interact at local vertices. One can argue similarly that [41] the only singularities of a BCFT two-point function lie on the light-cone and its reflection.

4 Time-like entanglement entropy in BCFT$_2$

In this section, we compute the time-like entanglement entropy for a time-like interval at zero and finite temperature in a two dimensional Lorentzian BCFT. We will do so by first computing the entanglement entropy for a generic interval in Euclidean signature followed by an analytical continuation to the Lorentzian signature to obtain the time-like entanglement entropy.

4.1 Zero temperature

Consider the configuration depicted in figure 1 for an interval $A \equiv [z_1, z_2] := [t_1, x_1), (t_2, x_2)]$ at zero temperature in a BCFT. The entanglement entropy for a generic space-like interval A in a BCFT$_2$ may be expressed in terms of twist field correlators using the replica technique [14, 15] as

$$S_A = \lim_{n\to 1}\frac{1}{1-n}\log\langle\sigma_n(z_1)\bar{\sigma}_n(z_2)\rangle\,, \tag{4.1}$$

where the scaling dimensions of the twist fields σ_n and $\bar{\sigma}_n$ are given by

$$\Delta_n = \bar{\Delta}_n = \frac{c}{12}\left(n - \frac{1}{n}\right). \tag{4.2}$$

We note that for a purely time-like interval A at a distance $x_1 = x_2$ from the boundary having time-like width $T_o = t_2 - t_1$, the cross-ratio which is given by

$$\xi = -\frac{T_0^2}{4x_1^2}\,, \tag{4.3}$$

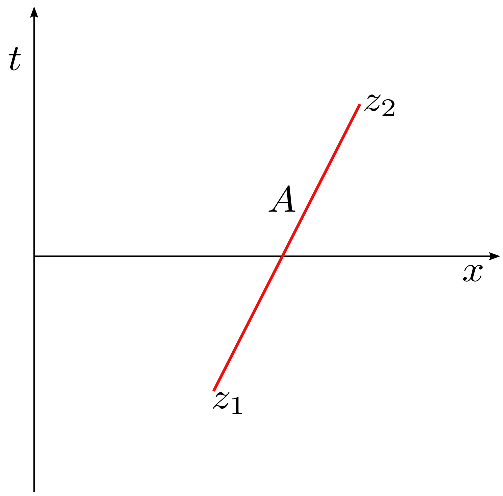

Figure 1. Schematic of a generic interval A in two dimensional BCFT.

is always negative. It is instructive to illustrate the different limits of ξ by following the value of T_0 with respect to x_1. When $T_0 \ll x_1$, we have $\xi \to 0^-$ and we are in the bulk limit. As T_0 increase and reaches the region of $2x_1$, one of the two points of the interval approaches the light cone of the image of the other point and we have the Regge limit $\xi \to -1$. Finally for $T_0 \gg x_1$, we arrive at the boundary limit $\xi \to -\infty$. This is different from the other boundary limit $\xi \to \infty$ which is obtained for a space-like interval. Let us now consider these limits in detail.

I. Bulk limit. Consider first the case that the interval is far away from the boundary such that $\xi \to 0$. In this case, the dominant contribution of the two point function comes from the bulk channel OPE. On utilizing the eq. (3.5), the two point twist in the bulk limit may be written in the following form

$$\langle \sigma_n(z_1)\bar{\sigma}_n(z_2)\rangle = \frac{\epsilon^{2\Delta_n}}{|z_1 - z_2|^{2\Delta_n}}, \tag{4.4}$$

where ϵ is a UV regulator. Now using the above eq. (4.4) in eq. (4.1), the entanglement entropy for a generic space-like interval A in the Lorentzian signature is given by

$$S_A = \frac{c}{3} \log \frac{\sqrt{(x_1 - x_2)^2 - (t_1 - t_2)^2}}{\epsilon} \tag{4.5}$$

For a purely time-like interval with $x_1 = x_2$, the time-like entanglement entropy S_A^T in the bulk limit is given by

$$S_A^T = \frac{c}{3} \log \frac{T_0}{\epsilon} + \frac{i\pi c}{6} := S^B, \tag{4.6}$$

where here the superscript B stands for the bulk. We observe that the time-like entanglement entropy is complex in this phase and resembles the usual CFT_2 result as given in eq. (2.2). Note that the standard entanglement entropy in a BCFT_2 also resembles the entanglement entropy of an interval in a CFT_2 in the bulk channel.

JHEP06(2023)173

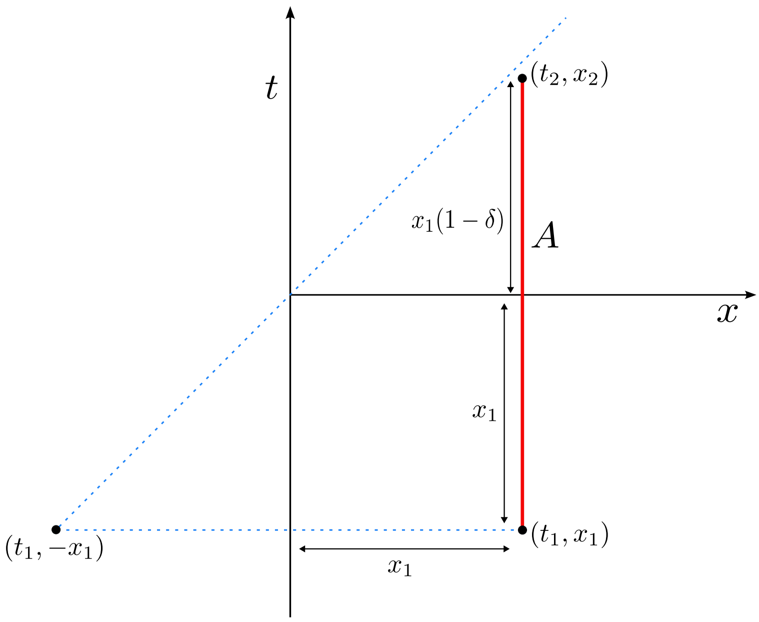

Figure 2. Schematic of a time-like interval in the Regge limit.

II. Regge limit. As T_0 increases, it will eventually reach the region $T_1 \approx 2x_1$. Let us parameterize the time interval by $T_0 = 2x_1(1-\delta/2)$. Due to time translational invariance, we can take the purely time-like interval as $A[(t_1, x_1), (t_2, x_2)] \equiv [(-x_1, x_1), (x_1(1-\delta), x_1)]$. See figure 2. In the leading order of small δ, the cross ratio ξ is given by

$$\xi = \frac{-(t_2 - t_1)^2 + (x_2 - x_1)^2}{4x_1 x_2} = -(1-\delta) \tag{4.7}$$

and the Regge limit is attained when the second end point of the interval proximate the light cone of the mirror image of the first end point of the interval. Using the two point function

$$\langle \sigma_n(z_1)\bar{\sigma}_n(z_2)\rangle = \frac{1}{|2x_1|^{2\Delta_n}} \frac{1}{(1+\xi)^{\Delta_n}}, \tag{4.8}$$

one obtains immediately the time-like entanglement entropy for the time-interval A in the Regge limit as

$$S_A^T = \begin{cases} \frac{c}{3}\log\left(\frac{2x_1}{\epsilon}\sqrt{2-\frac{T_0}{x_1}}\right), & \text{for } T_0 \to 2x_1^-, \quad \text{i.e. } \xi \to -1^+, \\ \frac{c}{3}\log\left(\frac{2x_1}{\epsilon}\sqrt{\frac{T_0}{x_1}-2}\right) + \frac{i\pi c}{6}, & \text{for } T_0 \to 2x_1^+, \quad \text{i.e. } \xi \to -1^-, \end{cases} := S^R, \tag{4.9}$$

where here the superscript R stands for Regge. Note that $\xi = -1$ is a branch point and this explain why S^R picks up an imaginary part as T_0 crosses the value of $2x_1$. Physically, the point z_2 has gone from the inside of the light-cone of the image point z_1' to the outside.

III. Boundary limit. In the boundary limit, the two point twist correlator may be expressed as

$$\langle \sigma_n(z_1)\bar{\sigma}_n(z_2)\rangle = \frac{g_b^{2(1-n)}\epsilon^{2\Delta_n}}{|4x_1 x_2|^{\Delta_n}}, \tag{4.10}$$

where $\mathcal{A} = g_b^{(1-n)}$ arises from the replica technique for BCFT entanglement entropy computations [16]. This gives the entanglement entropy for a generic interval A as

$$S_A = \frac{c}{6}\log\frac{2x_1}{\epsilon} + \frac{c}{6}\log\frac{2x_2}{\epsilon} + 2\log g_b, \tag{4.11}$$

where the second term describes the boundary entropy which depends on the boundary condition. Note that (4.11) is independent of the time t coordinate. Now taking $x_1 = x_2$ for a pure time-like interval, we obtain the time-like entanglement entropy

$$S_A^T = \frac{c}{3}\log\frac{2x_1}{\epsilon} + 2\log g_b := S^b, \tag{4.12}$$

where here the superscript b stands for the boundary. We see that the time-like entanglement entropy is real in this phase and includes boundary entropy which is expected in the boundary phase.

A couple of remarks are in order.

1. It is interesting that in contrast to the usual two phases of standard entanglement entropy in BCFT_2, we have a new phase of time-like entanglement entropy (4.9) which arises from the light-cone singularities. This is possible only for a time-like interval.

2. We remark that as the time-like entanglement entropy S_A^T is obtained by taking the log of the 2-point function (3.2) and $\mathcal{G}$ behaves as $\mathcal{G} \sim \xi^{-\Delta_n}, (1+\xi)^{-\Delta_n}$, constant $\mathcal{A}^2$ in the above said limits, it is clear that $S_A^T \sim \log\mathcal{G}$ picks up a non vanishing imaginary part in the bulk limit $\xi \to 0^-$ and in the time-like side of the Regge limit $1+\xi \to 0^-$, i.e $T_0 \gtrapprox 2x_1$.

3. It is instructive to follow the behavior of the time-like entanglement entropy and discuss its phase transition. Without loss of generality, consider fixed x_1 and let T_0 changes. For small T_0, S_A^T is given by S^B of (4.6). As T_0 increases, cross over from the bulk to the Regge behaviour occurs at:

$$S^B = S^R: \quad T_0 = 2(\sqrt{3}-1)x_1 := T_0^*, \tag{4.13}$$

where the equality of entropies is for the real part. As T_0 continue to increase, it eventually reaches the light-cone singularity point $T_0 \approx 2x_1$ and passes it. Crossover from the Regge behaviour to the boundary behaviour occurs at:

$$S^R = S^b: \quad T_0 = (2 + g_b^{12/c})x_1 := T_0^{**}. \tag{4.14}$$

One can show that $S_{bdy} \geq 0$ in an unitary BCFT and so $T_0^* < 2x_1 \leq T_0^{**}$. The behaviour of the time-like entropy curves is shown in figure 3.

4.2 Finite temperature

Next, let us compute the time-like entanglement entropy of an interval in two dimensional CFT on the half line at finite temperature β^{-1}. This can be obtained by computing the

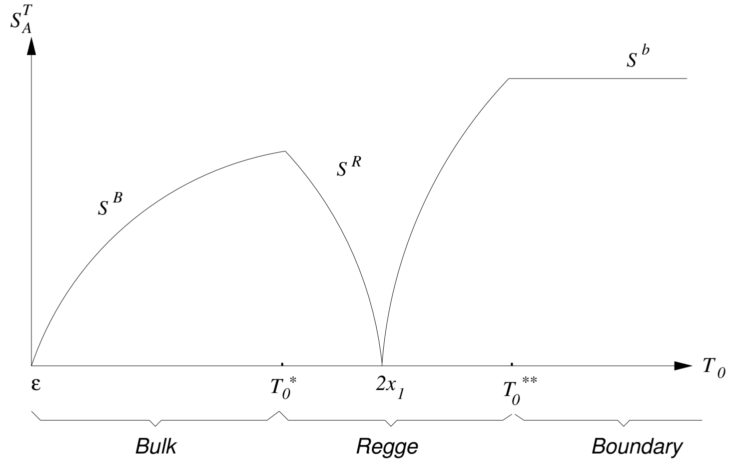

Figure 3. Phases of the time-like entanglement entropy S_A^T in BCFT.

two point twist correlation function on a half cylinder (with $w = x + i\tau, x \leq 0$) where the Euclidean time direction τ is compactified with period β. It is convenient to express it in terms of the two point function on the interior of the unit disc z via the conformal transformation $w \to z = e^{\frac{2\pi w}{\beta}}$:

$$\langle \sigma_n(w_1, \bar{w}_1)\bar{\sigma}_n(w_2, \bar{w}_2)\rangle_{\text{cyl}} = \prod_{i=1}^{2} \left(\frac{dz}{dw}\right)_{w=w_i}^{\Delta_n/2} \left(\frac{d\bar{z}}{d\bar{w}}\right)_{\bar{w}=\bar{w}_i}^{\bar{\Delta}_n/2} \langle \sigma_n(z_1, \bar{z}_1)\bar{\sigma}_n(z_2, \bar{z}_2)\rangle_{\text{disc}}\,, \quad (4.15)$$

where the two point function on the unit disk[4] of primary operators of dimensions Δ_1 and Δ_2 is given by [15, 43]

$$\langle \sigma_1(z_1, \bar{z}_1)\bar{\sigma}_2(z_2, \bar{z}_2)\rangle_{\text{disc}} = \frac{1}{(1 - z_1\bar{z}_1)^{\Delta_1}(1 - z_2\bar{z}_2)^{\Delta_2}}\mathcal{G}(\xi). \quad (4.16)$$

Here ξ is the cross ratio

$$\xi = \frac{|z_1 - z_2||\bar{z}_1 - \bar{z}_2|}{(1 - z_1\bar{z}_1)(1 - z_2\bar{z}_2)}. \quad (4.17)$$

and the function $\mathcal{G}(\xi)$ is known explicitly only in the bulk, boundary or Regge limit. The entanglement entropy for a generic interval $A = [w_1, w_2]$ on the cylinder is given by

$$S_A = \lim_{n\to 1} \frac{1}{1-n} \log \langle \sigma_n(w_1, \bar{w}_1)\bar{\sigma}_n(w_2, \bar{w}_2)\rangle_{\text{cyl}}\,. \quad (4.18)$$

As a result, we have three phases for the TEE at finite temperature similar to the zero temperature case.

I. Bulk limit. For this case when the interval is far away from the boundary, we have $\mathcal{G}(\xi) \sim \xi^{-\Delta_n}$ and hence

$$S_A = \frac{c}{6} \log\left[\left(\frac{\beta}{\pi\epsilon}\right)^2 \sinh\frac{\pi w_{12}}{\beta} \sinh\frac{\pi \bar{w}_{12}}{\beta}\right], \quad (4.19)$$

[4]The correlator on the unit disk can be obtained from the correlator on the upper half plane (UHP) through the Möbius transformation as $u = -i\left(\frac{z-1}{z+1}\right)$.

where $w_{12} = -x_{12} + i\tau_{12}$ and $\bar{w}_{12} = -x_{12} - i\tau_{12}$ are the interval length of A on the cylinder. Now analytically continue to the Lorentzian signature via $\tau \to it$, we have

$$S_A = \frac{c}{6} \log \left[\frac{1}{2} \left(\frac{\beta}{\pi \epsilon} \right)^2 (\cosh \frac{2\pi x_{12}}{\beta} - \cosh \frac{2\pi t_{12}}{\beta}) \right]. \tag{4.20}$$

Setting $x_{12} = 0$ and $t_{12} = T_0$, one obtain the time-like entanglement entropy for an interval A at finite temperature

$$S_A^T = \frac{c}{3} \log \left[\frac{\beta}{\pi \epsilon} \sinh \left(\frac{\pi T_0}{\beta} \right) \right] + \frac{i\pi c}{6}. \tag{4.21}$$

We observe that the above expression is same as the CFT result eq. (2.10) which is expected because the interval is far away from the boundary in this phase.

II. Regge limit. In the Regge limit, we have $\mathcal{G} \sim (1+\xi)^{-\Delta_n}$ and the finite temperature entanglement entropy for a generic interval in the Regge limit is given by

$$S_A = \frac{c}{6} \log \left[\left(\frac{\beta}{\pi \epsilon} \right)^2 \left(\sinh \frac{\pi(w_1 + \bar{w}_1)}{\beta} \sinh \frac{\pi(w_2 + \bar{w}_2)}{\beta} + \sinh \frac{\pi w_{12}}{\beta} \sinh \frac{\pi \bar{w}_{12}}{\beta} \right) \right]. \tag{4.22}$$

Analytically continuing to the Lorentzian signature via $\tau \to it$, we get the following time-like entanglement entropy of a generic time-like interval as

$$S_A = \frac{c}{6} \log \left[\left(\frac{\beta}{\pi \epsilon} \right)^2 \left(\sinh \frac{2\pi x_1}{\beta} \sinh \frac{2\pi x_2}{\beta} - \sinh \frac{\pi(x_{12} + t_{12})}{\beta} \sinh \frac{\pi(-x_{12} + t_{12})}{\beta} \right) \right]. \tag{4.23}$$

For a purely time like interval T_0 placed at a distance x_1 from the boundary, a light-cone singularity is reached when the second end point of the interval A approaches the mirror reflection of light cone of first point of the interval. Parameterize $T_0 = 2x_1(1 - \delta/2)$ as before, the time-like entanglement entropy for a time interval at finite temperature in the Regge limit is given by

$$S_A^T = \begin{cases} \frac{c}{6} \log \left(\frac{\beta(2x_1 - T_0)}{\pi \epsilon^2} \sinh \frac{4\pi x_1}{\beta} \right), & \text{for } T_0 \to 2x_1^-, \quad \text{i.e. } \xi \to -1^+, \\ \frac{c}{6} \log \left(\frac{\beta(T_0 - 2x_1)}{\pi \epsilon^2} \sinh \frac{4\pi x_1}{\beta} \right) + \frac{i\pi c}{6}, & \text{for } T_0 \to 2x_1^+, \quad \text{i.e. } \xi \to -1^-, \end{cases} := S^R. \tag{4.24}$$

Note that this has the correct zero temperature limit (4.9) as expected. Note also that the discontinuity of the imaginary part at the branch point is the same as in the zero temperature case.

III. Boundary limit. As the interval get close to the boundary, we have $\mathcal{G}(\xi) = g_b^{2(1-n)}$ in the UHP for the boundary limit and one obtains the entanglement entropy for a generic interval at finite temperature as

$$S_A = \frac{c}{6} \log \left[\left(\frac{\beta}{\pi \epsilon} \right)^2 \sinh \frac{\pi(w_1 + \bar{w}_1)}{\beta} \sinh \frac{\pi(w_2 + \bar{w}_2)}{\beta} \right] + 2 \log g_b. \tag{4.25}$$

Analytically continuing to the Lorentzian signature and take $w_1 + \bar{w}_1 = -2x_1$, $w_2 + \bar{w}_2 = -2x_2$ in the above expression we get

$$S_A = \frac{c}{6} \log \left[\left(\frac{\beta}{\pi \epsilon} \right)^2 \sinh \frac{2\pi x_1}{\beta} \sinh \frac{2\pi x_2}{\beta} \right] + 2 \log g_b. \tag{4.26}$$

Note that this is independent of the time coordinates. The time-like entanglement entropy for a purely time-like interval at finite temperature in this phase may now be obtained by taking $x_1 = x_2$ in eq. (4.26) and we obtain

$$S_A^T = \frac{c}{3} \log \left(\frac{\beta}{\pi \epsilon} \sinh \frac{2\pi x_1}{\beta} \right) + 2 \log g_b. \tag{4.27}$$

We observe that the time-like entanglement entropy is real in this phase unlike the previous phase.

One can similarly discuss the crossover of the entropies. The phase diagram is similar to the zero temperature case qualitatively except that the crossover position is now temperature dependent. We will omit the details here.

5 Holographic time-like entanglement entropy in $AdS_3/BCFT_2$

We now obtain the holographic time-like entanglement entropy in the context of $AdS_3/BCFT_2$ which involves the computation of bulk extremal curves (geodesics). We further show that the holographic TEE matches exactly with the dual field theory results.

5.1 AdS/BCFT duality

BCFTs [4, 6] describe physical systems with boundaries at the critical point. In addition to the traditional field theory techniques, a novel non-perturbative AdS/BCFT correspondence was originally introduced by Takayanagi [7] based on the idea of holography. At the level of classical gravity, the action for AdS/BCFT is given by

$$I = \frac{1}{16\pi G_N} \int_N d^{d+1}x \sqrt{|g|}(R - 2\Lambda) + \frac{1}{8\pi G_N} \int_Q d^d y \sqrt{|h|}(K - T), \tag{5.1}$$

where K is the extrinsic curvature, T is the tension of end-of-the-world (EOW) brane Q and h_{ij} is the induced metric on Q. The original proposal of Takayanagi [7] is to take on Q the Neumann boundary condition (NBC)

$$\text{NBC}: \ K^{ij} - (K - T)h^{ij} = 0. \tag{5.2}$$

The NBC imposes conditions on the end-of-the-world brane Q [7, 8, 44] as well as the bulk Einstein metric [45]. In addition to this, one may impose alternative boundary conditions for AdS/BCFT such as the conformal boundary condition (CBC) [9, 10] which fixes the conformal geometry and the trace of the extrinsic curvature of Q

$$\text{CBC}: \ K = \frac{d}{d-1} T. \tag{5.3}$$

One may also impose the Dirichlet boundary condition (DBC) [11], all of which define consistent theory of AdS/BCFT. For the special case of BCFT$_d$ on a half space, say $x \geq 0$, the bulk geometry is given by a portion of AdS$_{d+1}$. In the Poincaré coordinates (take AdS radius to be 1 for convenience)

$$ds^2 = \frac{1}{z^2}(dz^2 + dx_i^2)\,, \tag{5.4}$$

where the bulk geometry is given by a wedge with the EOW brane located at $x = z\sinh\rho_0$. Here ρ_0 is determined in term of the "tension" T as $T = (d-1)\tanh\rho_0$. Note that for flat boundary, all three BC give the same EOW brane [9–11]. However the holographic BCFT are still different in general as the spectrum of graviton fluctuations on the EOW brane is different for the different choice of BC. This, for example, results in different two point functions for the respective holographic BCFTs [46]. The existence of massive gravitons also leads to some puzzling behaviour for the island proposal as was pointed out originally in [47, 48].

Having reviewed about the AdS/BCFT duality, we now turn our attention to the computation of holographic time-like entanglement entropy for a time-like interval at zero and finite temperature in holographic BCFT$_2$.

5.2 Zero temperature

Consider a pure time-like interval A in the dual BCFT$_2$ at a fixed distance $x = x_1$ from the boundary. We have three possible choices of RT surface for this configuration depending on the size and distance from the boundary of an interval which are described below.

Phase I: bulk phase. In this phase, the interval is far away from the boundary such that the RT surface consists of two space-like geodesics and one time-like geodesic similar to section 2. This configuration is depicted in figure 4. So the holographic time-like entanglement entropy for an interval having length T_0 along the time direction in this phase may be expressed as

$$S_A^T = \frac{c}{3}\log\frac{T_0}{\epsilon} + \frac{i\pi c}{6}, \tag{5.5}$$

where the real part comes from the length of two hyperbola going to future infinity ($t = +\infty, z = +\infty$) and past infinity ($t = -\infty, z = +\infty$); and the imaginary part comes from the geodesic joining the future and past infinities. The above result agrees exactly with the corresponding dual BCFT$_2$ result eq. (4.6).

Phase II: Regge phase. For this phase, the end points of the purely time-like interval on the boundary can be parametrized as $A[(t_1, x_1), (t_2, x_2)] \equiv [(-x_1, x_1), (x_1(1-\delta), x_1)]$ with $\delta = 2 - T_0/x_1$. Consider first the case of $T_0 < 2x_1$ with $\delta > 0$. In this case, the RT surface is given by two geodesics where each geodesic joins the one end point of the interval and ends on the plane perpendicular to the boundary as shown in figure 5. The geodesics lie along the $t = \pm mx + c$ plane. The plane passing through the points (t_2, x_2) and mirror image of (t_1, x_1), i.e $(t_1, -x_1)$, is described by

$$t = mx + c, \quad m = 1 - \frac{\delta}{2}, \tag{5.6}$$

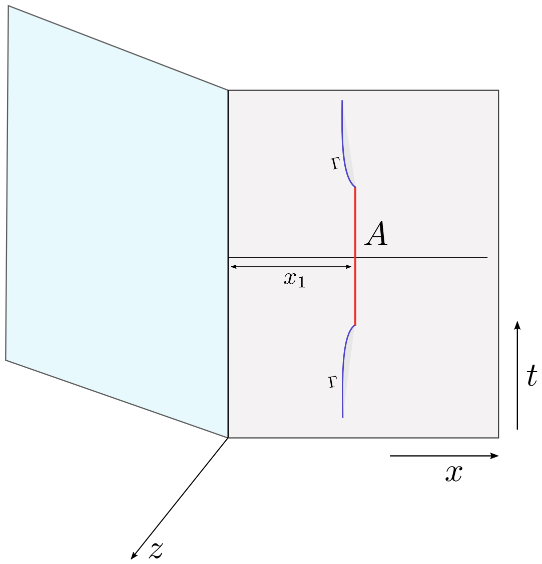

Figure 4. RT surfaces for configuration of a time-like interval in the bulk phase.

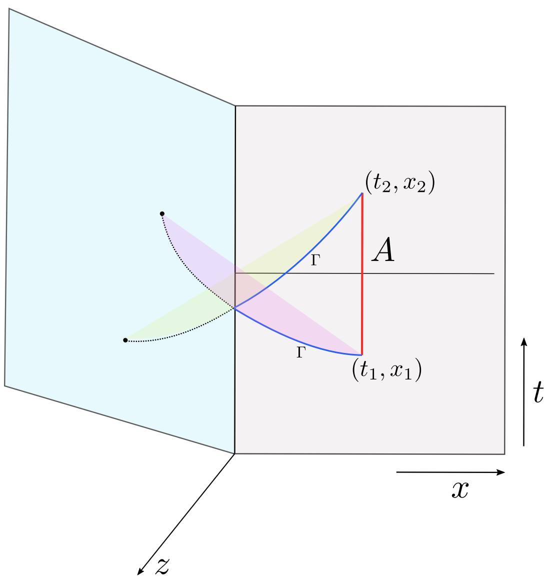

Figure 5. RT surfaces for configuration of a time-like interval in the Regge phase.

where m is the slope and c is some constant. The induced metric on this plane can be written as

$$\begin{aligned} ds^2 &= \frac{-dt^2 + dz^2 + dx^2}{z^2} = \frac{(1-m^2)dx^2 + dz^2}{z^2} \\ &= \frac{dy^2 + dz^2}{z^2}, \end{aligned} \tag{5.7}$$

JHEP06(2023)173

where we have defined $y = \sqrt{1-m^2}x$. Observe that the above metric in (y, z) coordinate looks like a time slice of AdS$_3$ geometry in Poincaré coordinates. So, the length of the geodesic Γ from the point (y_1, z_1) to a point on the perpendicular plane (y_2, z_2) (which is located at $x = 0$) along this plane is given by[5]

$$\begin{aligned} L &= \cosh^{-1}\left[\frac{(y_2-y_1)^2+z_1^2+z_2^2}{2z_1z_2}\right] \\ &\approx \log\left[\frac{\delta x_1^2+z^2}{\epsilon z}\right], \end{aligned} \tag{5.9}$$

where the point on the boundary and perpendicular plane is given by $(y_1, z_1) = (\sqrt{\delta}x_1, \epsilon)$ and $(y_2, z_2) = (0, z)$ respectively. After extremization of L with respect to z, we get the length of the geodesic as follows

$$L = \log\frac{2x_1\sqrt{\delta}}{\epsilon}. \tag{5.10}$$

The length of other geodesic which lie along the plane passing through the points (t_1, x_1) and $(t_2, -x_2)$ can be computed similarly and have the same length as L. So, we now obtain the holographic time-like entanglement entropy which is given by the sum of these two geodesics after using the RT formula as

$$S_A^T = \frac{c}{3}\log\left(\frac{2x_1}{\epsilon}\sqrt{2-\frac{T_0}{x_1}}\right). \tag{5.11}$$

This agrees precisely with the corresponding dual field theory result eq. (4.9). Similarly one can discuss the Regge limit from the other side $T_0 > 2x_1$ with $\delta < 0$. The computation is the same as above except now we have to take the negative root of the inverse cosh in eq. (5.9) for a time-like geodesic. As a result, we obtain the corresponding dual theory result (4.9) with the constant imaginary part. We remark that in field theory, the Regge phase of the TEE arises from the singular behaviour of the twist operator two point function in the Regge limit. On the gravity side, this arises from a particular RT geodesic which becomes null in the limit.

Phase III: boundary phase. Finally we consider the boundary phase where the interval is closer to the boundary. In this phase, the RT surface end on the brane as shown in figure 6. The length of each geodesic Γ which is at a constant time slice is given by [7]

$$L = \log\frac{2x_1}{\epsilon} + \rho_0, \tag{5.12}$$

where $\rho_0 = \tanh^{-1}(T)$. So the holographic time-like entanglement entropy for a time-like interval A may obtained using the RT formula as

$$S_A^T = \frac{c}{3}\log\frac{2x_1}{\epsilon} + \frac{c}{3}\rho_0, \tag{5.13}$$

[5]The geodesic distance between two points (t_1, x_1, z_1) and (t_2, x_2, z_2) in the Poincaré patch of AdS$_3$ is given by the standard formula

$$L = \cosh^{-1}\left[\frac{-(t_2-t_1)^2+(x_2-x_1)^2+z_1^2+z_2^2}{2z_1z_2}\right]. \tag{5.8}$$

JHEP06(2023)173

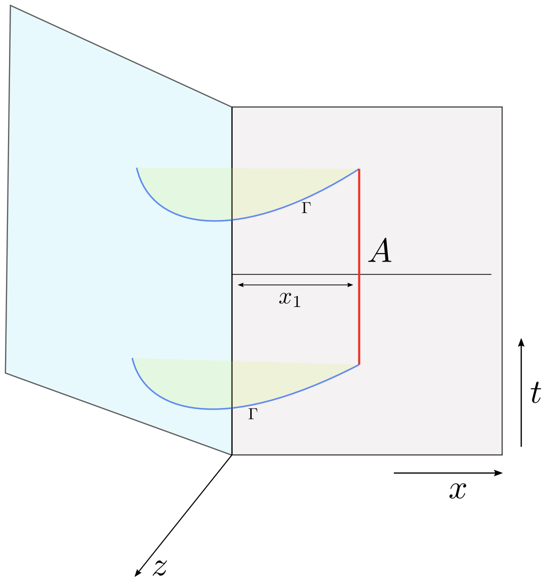

Figure 6. RT surfaces for configuration of a time-like interval in the boundary phase.

where the second term describes the boundary entropy [7]. It is $T \geq 0$ for unitary theory and so $S_{bdy} \geq 0$. We observe that the holographic time-like entanglement entropy in this phase also matches with dual BCFT result as described in eq. (4.12).

It is interesting to note that the topology of the RT surfaces are different for each of the three cases. This prompts us to interpret the crossover behaviour of entropies as phase transition of the entropies. Note that the bulk and boundary phases for the holographic time-like entropy is similar to the usual holographic entanglement entropy in $AdS_3/BCFT_2$. The bulk phase corresponds to the connected RT surface while the boundary phase corresponds to the disconnected RT surface. The appearance of the Regge phase is unique to the time-like entanglement entropy and is related to the existence of geodesics lying along the plane that joins one end point and the mirror reflection of other end point of the interval.

5.3 Finite temperature

We consider $BCFT_2$ in a half line at a finite temperature. In this case, the only known dual bulk solution is for $S_{bdy} = T = 0$ which is the BTZ black hole as described in eq. (2.9) truncated by a tensionless EOW brane perpendicular to the boundary along the $x = 0$ direction.[6] For a finite temperature BCFT on a half line with vanishing boundary entropy, we have three phase of the RT surface for the holographic time-like entropy which is similar to the zero temperature case, as follows.

[6]We note that for a general non-zero T, the holographic dual of a BCFT on an interval at finite temperature can be constructed by a part of two kind of bulk geometries i.e thermal AdS_3 and the BTZ black hole [7]. There exist a Hawking-Page transition at a certain temperature between these two geometries which depends on the brane tension. It would be interesting to obtain the TEE in this kind of setting which we leave to the future.

Phase I: bulk phase. In this phase, the RT surface consists of two space-like and one time-like extremal surface in a BTZ geometry similar to the CFT case as described in section 2. So, the holographic time-like entanglement entropy for a time-like interval of length T_0 in this phase is given by

$$S_A^T = \frac{c}{3}\log\left[\frac{\beta}{\pi\epsilon}\sinh\left(\frac{\pi}{\beta}T_0\right)\right] + \frac{i\pi c}{6}, \tag{5.14}$$

where the imaginary contribution comes from the time-like geodesic. The above TEE matches with the corresponding dual field theory result in eq. (4.21).

Phase II: Regge phase. For this phase, we have two RT surfaces with each geodesic connecting the end point of the interval and end on the perpendicular EOW brane, lying along the plane $t = mx + c$ similar to corresponding zero temperature case. Since the EOW brane is perpendicular to boundary, the length of each geodesic is half of the geodesic connecting the point (t_2, r_2, x_2) and mirror image of (t_1, r_1, x_1) which is $(t_1, r_1, -x_1)$. The geodesic length between two the points (t_1, r_1, x_1) and (t_2, r_2, x_2) in the BTZ black hole geometry can be expressed as

$$L = \cosh^{-1}\left[\frac{r_1 r_2}{r_+^2}\cosh r_+(x_2 - x_1) - \sqrt{\left(\frac{r_1^2}{r_+^2} - 1\right)}\sqrt{\left(\frac{r_2^2}{r_+^2} - 1\right)}\cosh r_+(t_2 - t_1)\right]. \tag{5.15}$$

The end point of the time-like interval A for this phase is given by $A[(t_1, r_1, x_1), (t_2, r_2, x_2)] \equiv [(-x_1, r_\infty, x_1), (x_1(1 - \delta), r_\infty, x_1)]$ with $T_0 = 2x_1(1 - \delta/2)$ for this configuration. Consider first the case $\delta > 0$, the length of geodesic connecting $(t_2, r_2, x_2) = (x_1(1 - \delta), r_\infty, x_1)$ and $(t_1, r_1, -x_1) = (-x_1, r_\infty, -x_1)$ can be obtained using the eq. (5.15) in the limit $\delta \to 0$ as

$$\begin{aligned} L &= \cosh^{-1}\left[\left(\frac{\beta r_\infty}{2\pi}\right)^2\cosh\frac{2\pi}{\beta}2x_1 - \left(\left(\frac{\beta r_\infty}{2\pi}\right)^2 - 1\right)\cosh\frac{2\pi}{\beta}(2x_1(1 - \delta/2))\right] \\ &= \log\left(\frac{\beta(2x_1 - T_0)}{\pi\epsilon^2}\sinh\frac{4\pi x_1}{\beta}\right), \end{aligned} \tag{5.16}$$

where $r_\infty \gg 1$ is related to the UV cut off as $r_\infty = 1/\epsilon$. Similarly, length of the geodesic connecting (t_1, r_1, x_1) and $(t_2, r_2, -x_2)$ gives the same (5.16). So the holographic time-like entanglement entropy for this phase may be obtained using the RT formula as $S_A^T = \frac{1}{4G_N}(\frac{L}{2} + \frac{L}{2})$ and

$$S_A^T = \frac{c}{6}\log\left(\frac{\beta(2x_1 - T_0)}{\pi\epsilon^2}\sinh\frac{4\pi x_1}{\beta}\right). \tag{5.17}$$

This result agrees exactly with the corresponding BCFT_2 result obtained in eq. (4.24). Similarly, one can consider approaching the Regge limit from the side of $T_0 > 2x_1$ with $\delta < 0$. The computation is the same as above and we obtain the corresponding dual theory result (4.24) with the constant imaginary part.

Phase III: boundary phase. Similar to the above discussion, we have two RT surfaces ending on the perpendicular EOW brane in phase II. The length of this geodesic connecting the interval and brane in a BTZ geometry can be obtained via mapping the BTZ geometry to the Poincaré patch of the AdS_3 space time as follows

$$L = \frac{1}{4G_N} \log\left(\frac{\beta}{\pi\epsilon} \sinh \frac{2\pi x_1}{\beta}\right), \tag{5.18}$$

where the pure time-like interval is located at $x = x_1$ distance from the boundary and the length of both geodesics are equal since they both lie at different time slice but at equal distance from the boundary. Then the holographic time-like entanglement entropy for an interval A can be obtained using the RT formula as

$$S_A^T = 2L = \frac{c}{3} \log\left(\frac{\beta}{\pi\epsilon} \sinh \frac{2\pi x_1}{\beta}\right). \tag{5.19}$$

It agrees with the corresponding dual field theory result in eq. (4.27) as $S_{bdy} = 0$.

6 Summary and discussion

To summarize, we have obtained the time-like entanglement entropy for a pure time-like interval in the context of $AdS_3/BCFT_2$. We first computed the time-like entanglement entropy in a $BCFT_2$ which involves the analytical continuation of the standard space-like entanglement entropy to a time-like interval. We observed that the TEE of a time-like interval at zero temperature has three phases in contrast to the two phases of the standard entanglement entropy in a BCFT. The new Regge phase is unique to the time-like interval when one end point of the interval approaches the light cone of the mirror reflection of other end point. We further computed the TEE of an interval on a half line at a finite temperature and found that it has similar three phases. The TEE has a constant and temperature independent imaginary part in the bulk limit of small T_0 and in the Regge limit of $T_0 \to 2x_1^+$, and is otherwise real.

Subsequently, we computed the time-like entanglement entropy for a time-like interval holographically from the bulk dual to the zero and finite temperature $BCFT_2$. This involves the computation of RT surface (extremal curves) in the bulk geometry. For the zero temperature case, the bulk dual is described by a part of the AdS_3 geometry truncated by an EOW brane. It is observed that the holographic TEE is described by three choices of the RT surface. The bulk and the boundary phases consists of connected and disconnected RT surface which is similar to the usual holographic entanglement entropy cases. The RT surface for the Regge phase is obtained by considering the two geodesics that go along the plane joining one end point and the mirror reflection of the other end point of the interval. These two geodesics meet at the plane perpendicular to the boundary and join together to form the desired RT surface. We also considered the finite temperature case where the bulk dual is BTZ black hole cut off by a perpendicular tensionless EOW brane and observed that it also has three phases. Interestingly, we observed that the holographic TEE agrees precisely with the dual field theory results at both zero and finite temperature cases in the gravity approximation.

In this paper, we find interesting phase structure for the TEE in BCFT. However, a basic definition of TEE directly in terms of the field theory Hilbert space without employing analytic continuation or holographic minimal surfaces is lacking. It is interesting to consider concrete example of quantum system and try to demonstrate the physical relevance of TEE. As such, we note that physically the pure time interval in $BCFT_2$ describes the configuration of a quantum dot on a half line. Our results for the TEE should describe some kind of entanglement of a partial history of the dot with it's complement. As the quantum dot is an easily accessible system, one may be able to observe discontinuity for some measurables at the transition points identified from the phase diagram of TEE. This will give a possible demonstration of the physical relevance of the TEE.

Previously, it has been argued that the TEE in CFT can be properly understood as a pseudo entropy. It will be interesting to consider this generalization properly to clarify the connection of TEE in a BCFT with the pseudo entropy. It will also be extremely interesting to explore the island formalism for TEE in the context of Island/BCFT correspondence along the lines of [49–51]. The study of time-like entanglement entropy is expected to shed new insights in our understanding of the black hole interior and the emergence of spacetime geometry from quantum entanglement. We note that the signature for an asymptotic observer get swapped as one passes the horizon which suggests that the time-like entropy may play an important role in the understanding of quantum entanglement in the interior of the black hole. We leave these interesting issue for future investigations.

Acknowledgments

We thank Jaydeep Kumar Basak, Adrita Chakraborty and Dimitris Giataganas for helpful discussion. We acknowledge support of this work by NCTS and the grant 110-2112-M-007-015-MY3 of the National Science and Technology Council of Taiwan.

References

[1] J.M. Maldacena, *The large N limit of superconformal field theories and supergravity*, *Adv. Theor. Math. Phys.* **2** (1998) 231 [hep-th/9711200] [INSPIRE].

[2] J.L. Cardy, *Conformal invariance and surface critical behavior*, *Nucl. Phys. B* **240** (1984) 514 [INSPIRE].

[3] J.L. Cardy, *Boundary conditions, fusion rules and the Verlinde formula*, *Nucl. Phys. B* **324** (1989) 581 [INSPIRE].

[4] D.M. McAvity and H. Osborn, *Energy momentum tensor in conformal field theories near a boundary*, *Nucl. Phys. B* **406** (1993) 655 [hep-th/9302068] [INSPIRE].

[5] D.M. McAvity and H. Osborn, *Conformal field theories near a boundary in general dimensions*, *Nucl. Phys. B* **455** (1995) 522 [cond-mat/9505127] [INSPIRE].

[6] J.L. Cardy, *Boundary conformal field theory*, hep-th/0411189 [INSPIRE].

[7] T. Takayanagi, *Holographic dual of BCFT*, Phys. Rev. Lett. **107** (2011) 101602 [arXiv:1105.5165] [INSPIRE].

[8] M. Fujita, T. Takayanagi and E. Tonni, *Aspects of AdS/BCFT*, JHEP **11** (2011) 043 [arXiv:1108.5152] [INSPIRE].

[9] R.-X. Miao, C.-S. Chu and W.-Z. Guo, *New proposal for a holographic boundary conformal field theory*, Phys. Rev. D **96** (2017) 046005 [arXiv:1701.04275] [INSPIRE].

[10] C.-S. Chu, R.-X. Miao and W.-Z. Guo, *On new proposal for holographic BCFT*, JHEP **04** (2017) 089 [arXiv:1701.07202] [INSPIRE].

[11] R.-X. Miao, *Holographic BCFT with Dirichlet boundary condition*, JHEP **02** (2019) 025 [arXiv:1806.10777] [INSPIRE].

[12] S. Ryu and T. Takayanagi, *Holographic derivation of entanglement entropy from AdS/CFT*, Phys. Rev. Lett. **96** (2006) 181602 [hep-th/0603001] [INSPIRE].

[13] S. Ryu and T. Takayanagi, *Aspects of holographic entanglement entropy*, JHEP **08** (2006) 045 [hep-th/0605073] [INSPIRE].

[14] P. Calabrese and J.L. Cardy, *Entanglement entropy and quantum field theory*, J. Stat. Mech. **0406** (2004) P06002 [hep-th/0405152] [INSPIRE].

[15] P. Calabrese and J. Cardy, *Entanglement entropy and conformal field theory*, J. Phys. A **42** (2009) 504005 [arXiv:0905.4013] [INSPIRE].

[16] J. Sully, M. Van Raamsdonk and D. Wakeham, *BCFT entanglement entropy at large central charge and the black hole interior*, JHEP **03** (2021) 167 [arXiv:2004.13088] [INSPIRE].

[17] K. Doi et al., *Pseudoentropy in dS/CFT and timelike entanglement entropy*, Phys. Rev. Lett. **130** (2023) 031601 [arXiv:2210.09457] [INSPIRE].

[18] P. Wang, H. Wu and H. Yang, *Fix the dual geometries of $T\bar{T}$ deformed CFT_2 and highly excited states of CFT_2*, Eur. Phys. J. C **80** (2020) 1117 [arXiv:1811.07758] [INSPIRE].

[19] K. Doi et al., *Timelike entanglement entropy*, JHEP **05** (2023) 052 [arXiv:2302.11695] [INSPIRE].

[20] Y. Nakata et al., *New holographic generalization of entanglement entropy*, Phys. Rev. D **103** (2021) 026005 [arXiv:2005.13801] [INSPIRE].

[21] A. Mollabashi et al., *Pseudo entropy in free quantum field theories*, Phys. Rev. Lett. **126** (2021) 081601 [arXiv:2011.09648] [INSPIRE].

[22] A. Mollabashi et al., *Aspects of pseudoentropy in field theories*, Phys. Rev. Res. **3** (2021) 033254 [arXiv:2106.03118] [INSPIRE].

[23] B. Liu, H. Chen and B. Lian, *Entanglement entropy in timelike slices: a free fermion study*, arXiv:2210.03134 [INSPIRE].

[24] N.L. Diaz, J.M. Matera and R. Rossignoli, *Path integrals from spacetime quantum actions*, arXiv:2111.05383 [INSPIRE].

[25] W.-Z. Guo, S. He and Y.-X. Zhang, *Constructible reality condition of pseudo entropy via pseudo-Hermiticity*, JHEP **05** (2023) 021 [arXiv:2209.07308] [INSPIRE].

[26] L. Aalsma, S.E. Aguilar-Gutierrez and W. Sybesma, *An outsider's perspective on information recovery in de Sitter space*, JHEP **01** (2023) 129 [arXiv:2210.12176] [INSPIRE].

JHEP06(2023)173

[27] K. Narayan, *De Sitter space, extremal surfaces, and time entanglement*, *Phys. Rev. D* **107** (2023) 126004 [arXiv:2210.12963] [INSPIRE].

[28] K.S. Reddy, *A timelike entangled island at the initial singularity in a JT FLRW ($\Lambda > 0$) universe*, arXiv:2211.14893 [INSPIRE].

[29] Z. Li, Z.-Q. Xiao and R.-Q. Yang, *On holographic time-like entanglement entropy*, *JHEP* **04** (2023) 004 [arXiv:2211.14883] [INSPIRE].

[30] A.J. Parzygnat and J. Fullwood, *From time-reversal symmetry to quantum Bayes' rules*, *PRX Quantum* **4** (2023) 020334 [arXiv:2212.08088] [INSPIRE].

[31] S. He, J. Yang, Y.-X. Zhang and Z.-X. Zhao, *Pseudo-entropy for descendant operators in two-dimensional conformal field theories*, arXiv:2301.04891 [INSPIRE].

[32] H. Alshal, *Einstein's equations and the entropy of pseudo-Riemannian information manifolds*, arXiv:2301.13017 [INSPIRE].

[33] J. Cotler and A. Strominger, *Cosmic ER=EPR in dS/CFT*, arXiv:2302.00632 [INSPIRE].

[34] H.-Y. Chen, Y. Hikida, Y. Taki and T. Uetoko, *Complex saddles of three-dimensional de Sitter gravity via holography*, *Phys. Rev. D* **107** (2023) L101902 [arXiv:2302.09219] [INSPIRE].

[35] Z. Chen, *Complex-valued holographic pseudo entropy via real-time AdS/CFT correspondence*, arXiv:2302.14303 [INSPIRE].

[36] X. Jiang, P. Wang, H. Wu and H. Yang, *Timelike entanglement entropy and $T\bar{T}$ deformation*, arXiv:2302.13872 [INSPIRE].

[37] K. Narayan and H.K. Saini, *Notes on time entanglement and pseudo-entropy*, arXiv:2303.01307 [INSPIRE].

[38] X. Jiang, P. Wang, H. Wu and H. Yang, *Timelike entanglement entropy in dS_3/CFT_2*, arXiv:2304.10376 [INSPIRE].

[39] D. Mazáč, L. Rastelli and X. Zhou, *An analytic approach to $BCFT_d$*, *JHEP* **12** (2019) 004 [arXiv:1812.09314] [INSPIRE].

[40] J.D. Brown and M. Henneaux, *Central charges in the canonical realization of asymptotic symmetries: an example from three-dimensional gravity*, *Commun. Math. Phys.* **104** (1986) 207 [INSPIRE].

[41] W. Reeves et al., *Looking for (and not finding) a bulk brane*, *JHEP* **12** (2021) 002 [arXiv:2108.10345] [INSPIRE].

[42] J. Maldacena, D. Simmons-Duffin and A. Zhiboedov, *Looking for a bulk point*, *JHEP* **01** (2017) 013 [arXiv:1509.03612] [INSPIRE].

[43] P. Calabrese, J. Cardy and E. Tonni, *Finite temperature entanglement negativity in conformal field theory*, *J. Phys. A* **48** (2015) 015006 [arXiv:1408.3043] [INSPIRE].

[44] M. Nozaki, T. Takayanagi and T. Ugajin, *Central charges for BCFTs and holography*, *JHEP* **06** (2012) 066 [arXiv:1205.1573] [INSPIRE].

[45] R.-X. Miao and C.-S. Chu, *Universality for shape dependence of Casimir effects from Weyl anomaly*, *JHEP* **03** (2018) 046 [arXiv:1706.09652] [INSPIRE].

[46] C.-S. Chu and R.-X. Miao, *Conformal boundary condition and massive gravitons in AdS/BCFT*, *JHEP* **01** (2022) 084 [arXiv:2110.03159] [INSPIRE].

[47] H. Geng et al., *Information transfer with a gravitating bath*, *SciPost Phys.* **10** (2021) 103 [arXiv:2012.04671] [INSPIRE].

[48] H. Geng et al., *Inconsistency of islands in theories with long-range gravity*, *JHEP* **01** (2022) 182 [arXiv:2107.03390] [INSPIRE].

[49] K. Suzuki and T. Takayanagi, *BCFT and islands in two dimensions*, *JHEP* **06** (2022) 095 [arXiv:2202.08462] [INSPIRE].

[50] Y.-K. Suzuki and S. Terashima, *On the dynamics in the AdS/BCFT correspondence*, *JHEP* **09** (2022) 103 [arXiv:2205.10600] [INSPIRE].

[51] K. Izumi et al., *Brane dynamics of holographic BCFTs*, *JHEP* **10** (2022) 050 [arXiv:2205.15500] [INSPIRE].

JHEP06(2023)173